CHARACTERIZING URBAN VEHICLE TEST COURSES BY THEIR POWER SPECTRA

Dr. Andrew W. Harrell*, John G. Green Mobility Systems Branch, Geotechnical and Structures Laboratory, Engineering Research and Development Center (ERDC),Vicksburg, MS 39180

This paper will discuss various ways to use wavelet detrending parameters to learn and identify patterns in power spectra. ERDC vehicle ride courses with urban obstacles were analyzed in terms of different time averaged, or windowed, Fourier transform formulas in order to characterize the spectra of their elevation profiles. Simulation results of the High Mobility Multi-purpose Wheeled Vehicle (HMMMV) on two different test courses, both with nearly the same root mean square (RMS) variation, have been found to generate different power spectra response characteristics in test vehicles. The Vehdyn mathematical model that was used for parallel simulations, models a test vehicle's response as being primarily due to the RMS of the test course. In these simulations the spacing of the bumps was found to generate different power spectral characteristics in different test courses with the same RMS. Thus, improving the theoretical understanding of how to characterize the power spectra of the courses should give us new and better ways to improve and validate our modeling. For instance, we expect to see this in terms of developing a better understanding of the effects of the surface geometry in urban terrain with sharp discontinuities such as potholes and obstacles on military vehicles.

Purpose

The purpose of the research reported in this paper is threefold: (1) to assist the ERDC in quantifying urban terrain for generating performance analysis with current data sets, (2) to develop methodology to supply representative urban terrain for vehicle dynamic analysis and simulators, (3) explain mathematical methodology and the approach to the analysis which was used in this study and which can accomplish in the future the first two objectives.

Background

ERDC's Mobility Systems Branch has been conducting vehicle ride tests for many years. So the idea of performing vehicle ride tests is nothing new. However, most of the ride tests in the past have been conducted in off-road/cross country situations on natural or simulated natural terrain. There has been very little research into vehicle ride performance in degraded urban terrain consisting of rubble and scattered debris. As a starting point, a paved section of road located at the ERDC-Vicksburg Test Track was utilized to perform multiple vehicle ride tests. The following sections will describe how these tests were setup and carried out.

Test Vehicles

Three military vehicles were selected for these tests. The Army's High Mobility Multipurpose Wheeled Vehicle (HMMWV) and the M2 Bradley tracked vehicle, and a wheeled Marine Corps prototype vehicle called the Helo-Transportable Tactical Vehicle (HTTV).

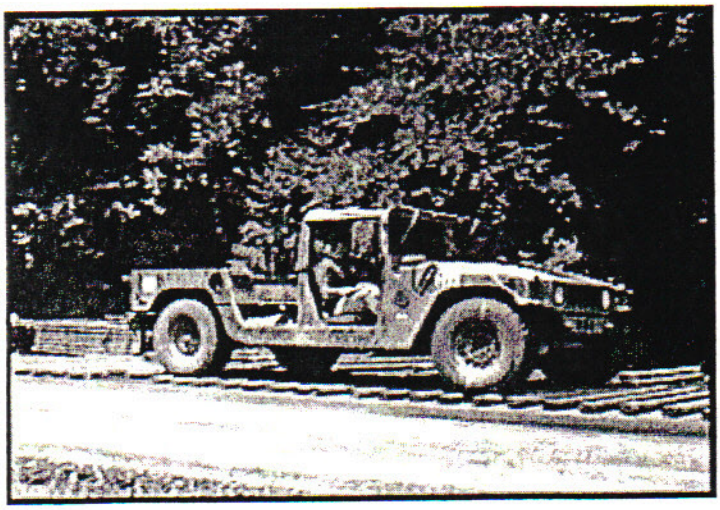

Figure 1. HMMWV Test Vehicle.

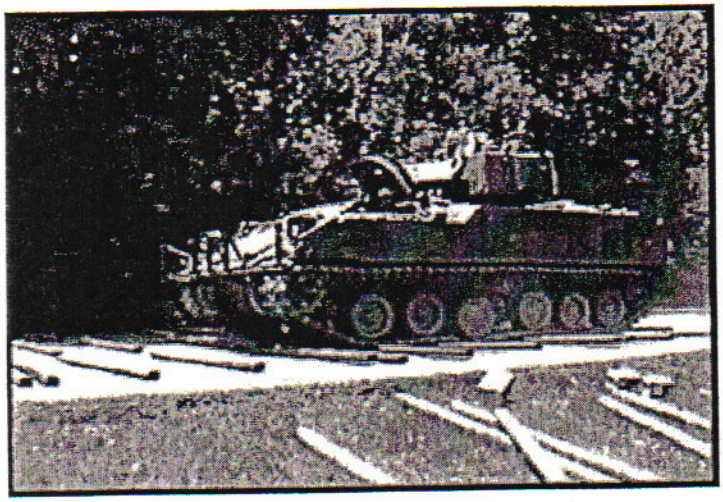

Figure 2. M2 Test Vehicle.

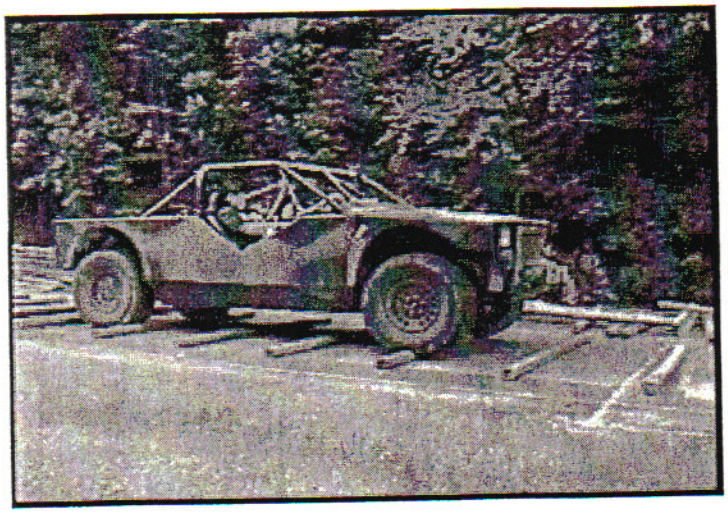

Figure 3. HTTV Test Vehicle.

Test Course Layout

A section of paved road 250 feet long was selected at the ERDC Vicksburg Test Track to simulate an urban environment. The actual course was 100 feet long and 20 feet wide. For these tests, 8 feet landscape timbers were used to simulate urban rubble and debris. These timbers were laid out in several different course configurations including 1, 2, 3, and 4 feet evenly spaced, staggered spaced, and randomly spaced. For both the evenly and randomly spaced courses, a single column of timbers was used for the HMMWV and HTTV tests because these vehicles are less than 8 feet wide. For the staggered spaced courses, two columns of offset timbers were used for the HMMWV and HTTV. Two columns of timbers were used for all the M2 tests due to the width of the vehicle. An example of one of the test courses is shown in figure 4.

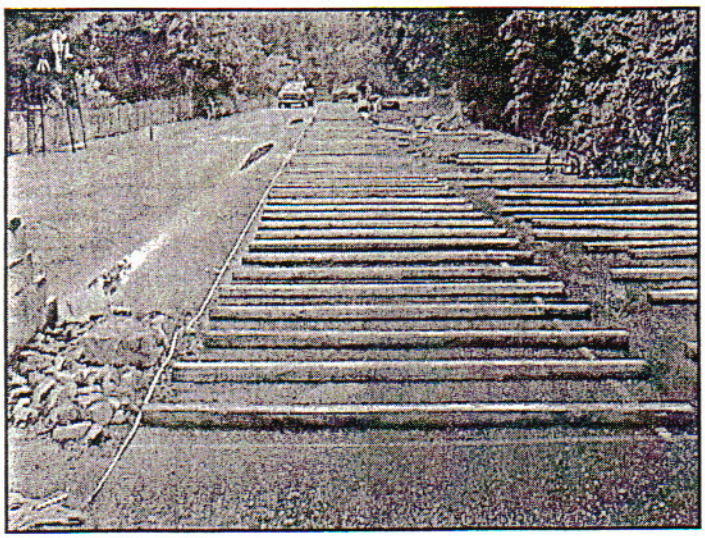

Figure 4. Example of Test Course.

Test Course Runs

Vehicle ride tests were conducted using vehicles instrumented with the Waterways Experiment Station (WES) ride/shock meter. The ride/shock meters are connected to accelerometers which are connected to the point on the vehicle from which measurements are desired. These meters measure the absorbed power (ride) and the peak vertical acceleration (shock) of the vehicle component on which the accelerometer is located. For each of the study ride tests, two ride/shock meters and accelerometers were used. The accelerometers were tethered to each ride meter and were attached to two different locations on the vehicle; one underneath the driver's seat and one on the driver's seat. The ride/shock meters measured both the absorbed power and peak vertical acceleration of the

Absorbed power is measured in wattage units while peak vertical acceleration is measured in g's. Typically, there are three levels of absorbed power considered in vehicle mobility modeling and analysis; 6, 9, and 12 watts. 6 watts is loosely defined as the ride limit that a driver can sustain for a time period of about 8 hours. 9 watts is the ride limit that a driver can sustain for about 1 hour, and 12 watts is the ride limit that a driver can sustain for only about 5 minutes. For vehicle shock, typically, 2.5 g's is the driver limit. In the past, relationships were developed from vehicle ride tests which related the vehicle ride to a number representative of the terrain roughness. This number is the detrended root mean square (rms) of the ride course shifted to a mean of zero. Detrending is a methodology of averaging at given distance intervals to take out the effects of low frequency events on the course.

Test Course Results

One thing that was obvious with all vehicle tests was that 1 foot evenly spaced, non-staggered timbers had a bridging affect which resulted in high vehicle speeds and low wattages. Tests with 2', 3', and 4' evenly-spaced, non-staggered timbers resulted in low vehicle speeds and high wattages. Another thing noticed was that the test vehicles with highway tire pressure did not perform as well as the same vehicle with cross country tire pressure. This can be explained by the fact the cross country tire pressure

was lower than the highway tire pressure which meant that the cross country tire pressure provided more of a cushion to the vehicle.

VEHDYN Module

Overview

The ERDC's Vehicle Dynamics Module, referred to as VEHDYN, was developed by the Waterways Experiment Station (WES) in 1974 (Murphy and Ahlvin 1976) to provide ride and shock simulation capability for general use in support of the Army Mobility Model (AMM). VEHDYN's primary purpose was to predict the gross motion of a vehicle chassis en negotiating rough terrain or discrete obstacles and to calculate the resulting absorbed power (a ride comfort criterion) or largest peak acceleration (shock criterion) from the vertical accelerations at a specified location in the vehicle. The VEHDYN predictions are used to calculate ride- and shock-limiting speeds (the speeds at which 6 watts absorbed power or peak accelerations of 2.5 g's occur) as a function of terrain roughness or obstacle height (Creighton 1986).

VEHDYN is a FORTRAN computer code that performs dynamics analysis of a vehicle system's interaction with a given terrain profile. The terrain profile is simply a file that contains the *(x,y)* coordinates of the representative terrain or discrete obstacle. In order to run VEHDYN three data files are required; the control parameters file, the terrain profile, and the vehicle file.

The control parameters data file contains the information that describes how the run will proceed. It includes descriptors to select a particular vehicle and a particular terrain profile, vehicle velocity, integration time step, run length, output time increments for each of three output files, and frequency for the low-pass filter for the absorbed power calculation (Creighton 1994). The terrain profile data files defines a two-dimensional rigid, nondeformable surface over which the vehicle travels during the course of the VEHDYN run. The vehicle data file contains enough information so that VEHDYN can recreate the vehicle in a known configuration, specifically, an equilibrium, or settled, configuration.

Urban Terrain Profiles

As mentioned, VEHDYN has primarily been used on rough terrain (off-road, cross country terrain) and discrete obstacles which may be either off- or on-road. The terrain in a degraded urban environment can consist of many small discrete obstacles on top of a road or street. In order to create virtual urban terrain profiles, the material type, size, and spacing or distribution had to be considered. The material types defined in the Environmental Data Model (EDM) for urban rubble were used as a basis for determining these discrete obstacles. These types are based on the construction material types for buildings that would be found in an urban environment. They include CONCRETE, GLASS, MASONRY, STEEL, VINYL SIDING, and WOOD. A FORTRAN computer code was written to generate the virtual urban terrain profiles in which the discrete obstacles were sized based on the typical size for each of the material types. The sizes used were 1" for GLASS, 2" for VINYL SIDING, 2.5" for MASONRY, 3" FOR WOOD, 5" for CONCRETE, and 8" for STEEL. The data format of these files can be seen in the sample file shown in Appendix D. In order to fill in data gaps, a 4" and 6" obstacle size were also used. The distribution or spacing of these obstacles was also considered with 1', 2', 3', 4', 5', and 6' spacing modeled. Lastly, to account for the variability that might occur in the rubble and debris in the degraded urban environment, a variability in the material size and spacing was included in the profile generation. The values used for the variability were 0%, 25%, 50%, 75%, and 100%, and refer to the amount of variability given to each obstacle's height and spacing.

The individual obstacles were modeled as half-rounds with the radius being the height of the various material types. With this information, 240 urban terrain profiles were generated. The profiles with non-zero variability were uniformly, randomly generated given the base obstacle height and spacing. Each of these profiles was made 200' in length because historically vehicle ride tests have been made on courses 200' or longer. As an example, figure 5 and 6 show sections of two of the urban terrain profiles; CONCRETE at 1 foot spacing with 0% variability, and WOOD at 1 foot spacing with 75% variability, respectively.

Module Runs

Output of a VEHDYN module run includes, among other things, the average absorbed power or wattage and the peak vertical acceleration for a given vehicle on a terrain profile at a given vehicle speed. In order to hone in on the 6, 9, and 12 watt speeds for a vehicle, multiple runs at various speeds must be made for each vehicle and terrain profile. The vehicle speeds used in our study were in increments of 2 mph starting at 2 mph up to 20 mph. Then the speed increment was increased to 5 mph up to the max vehicle speed. On average, 3000 module runs were made for each of the study vehicles used for a total of approximately 15,000 module runs. There is also a VEHDYN animation program that can be used to visually inspect a vehicle's reaction to the terrain on which it rides. Figures 10 thru 13 show screenshots from this animation program; figures 7 and 8 show the HMMWV on the two urban terrain profiles that were shown in figures 5 and 6., and figure 9 shows the Kawasaki 650 ATV on another profile.

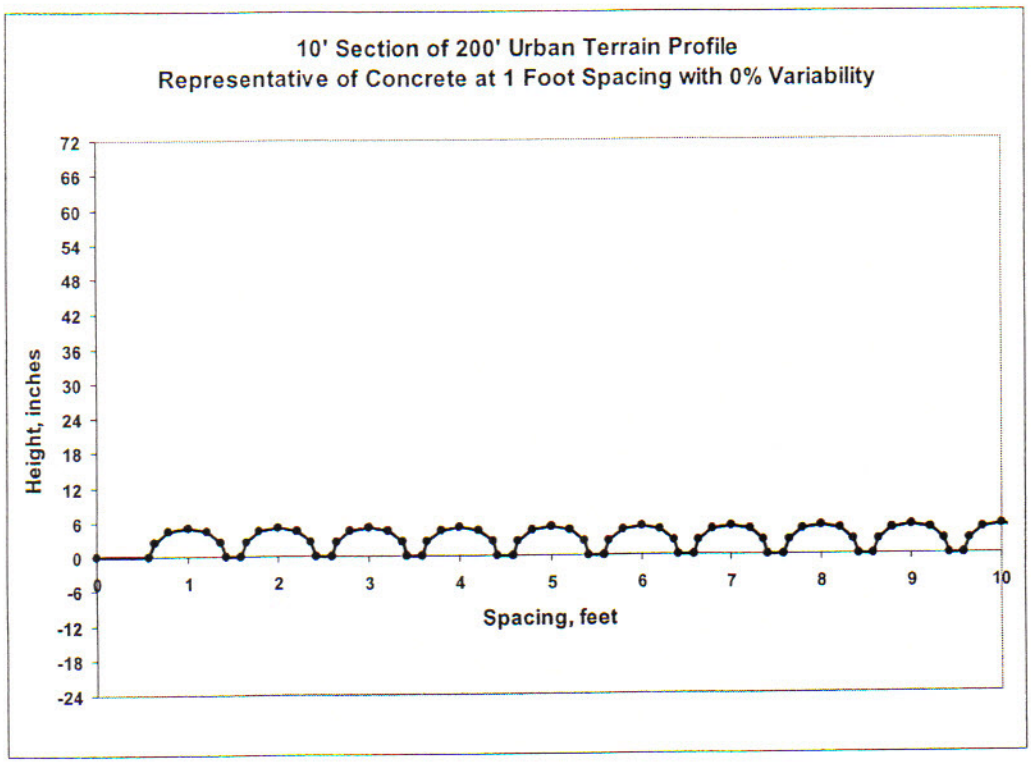

Figure 5. Example of Plotted Urban Terrain Profile Data.

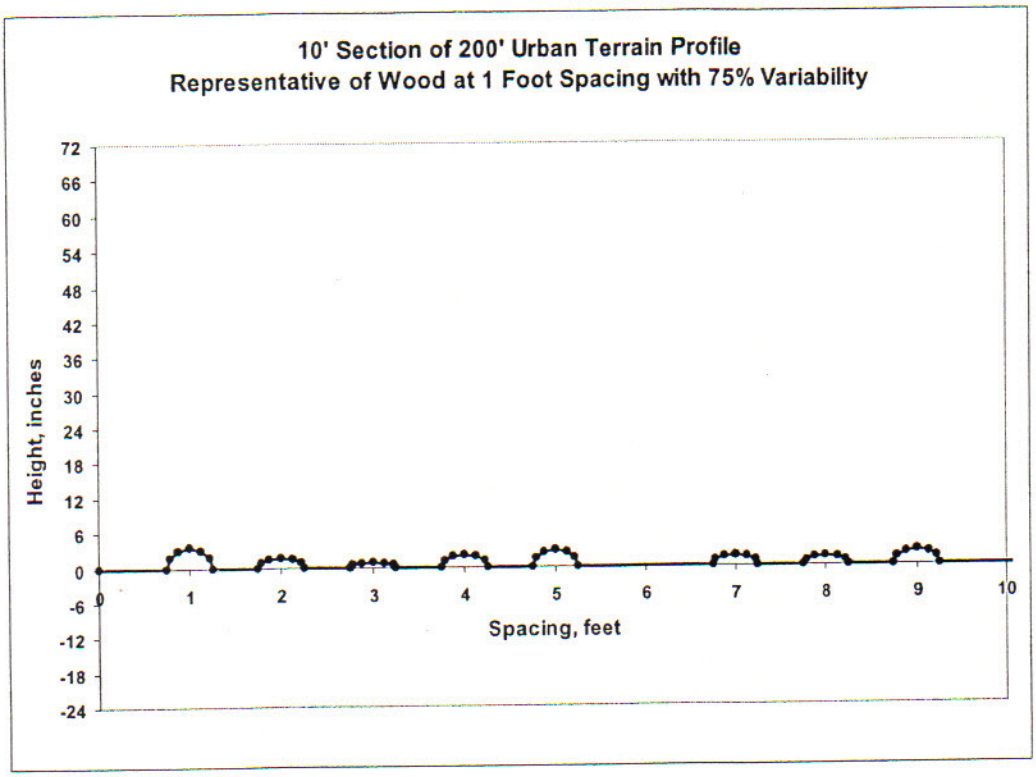

Figure 6. Example of Plotted Urban Terrain Profile Data.

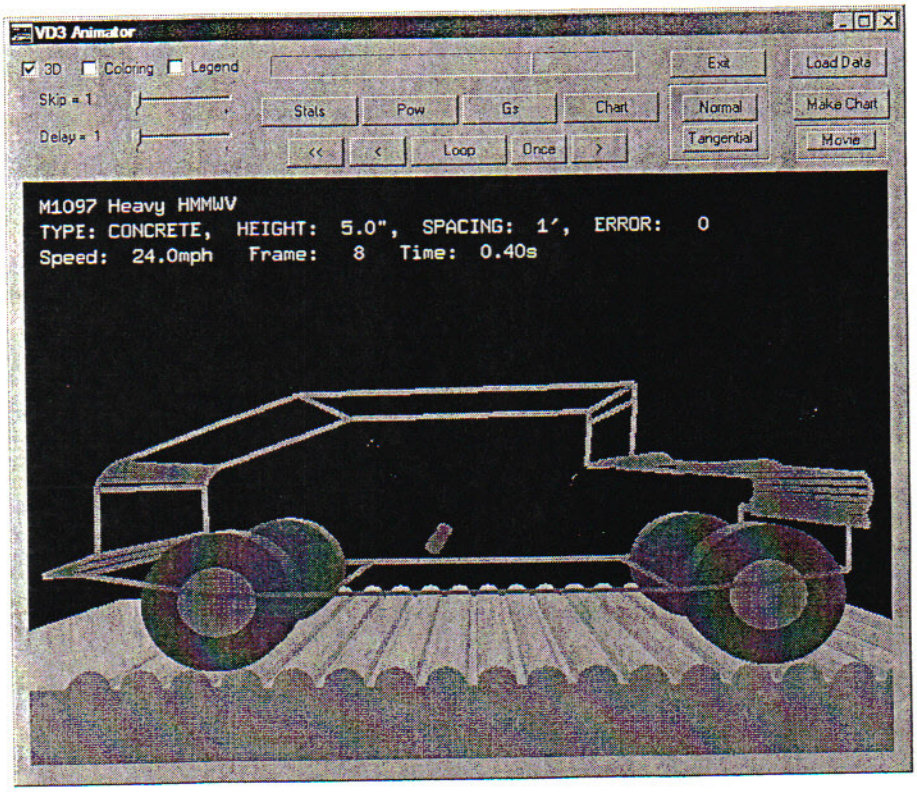

Figure 7. VEHDYN Animation of a HMMWV.

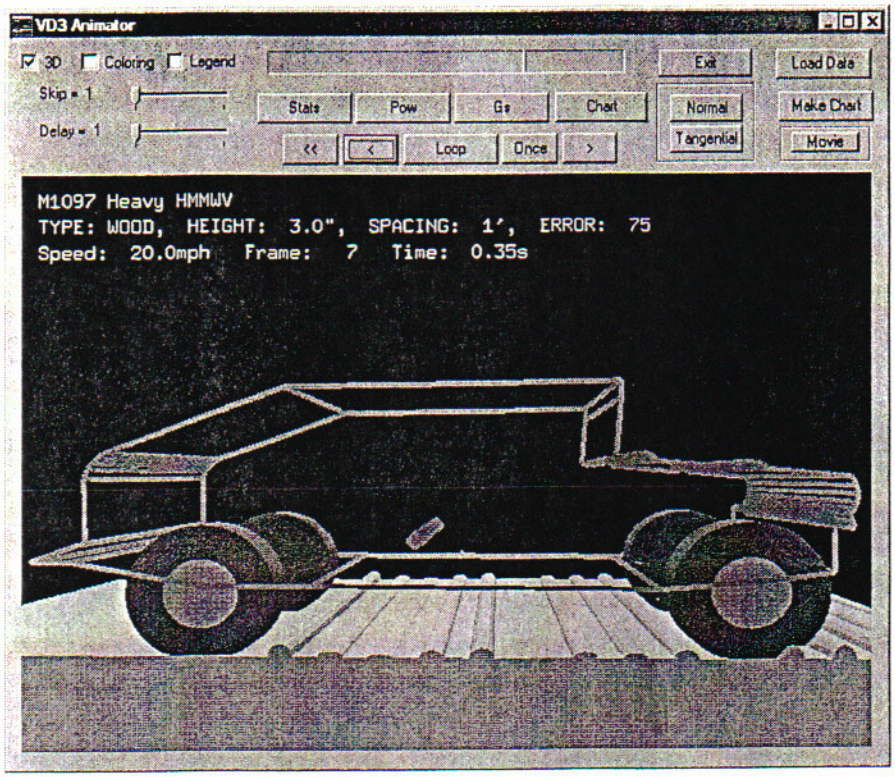

Figure 8. VEHDYN Animation of a HMMWV.

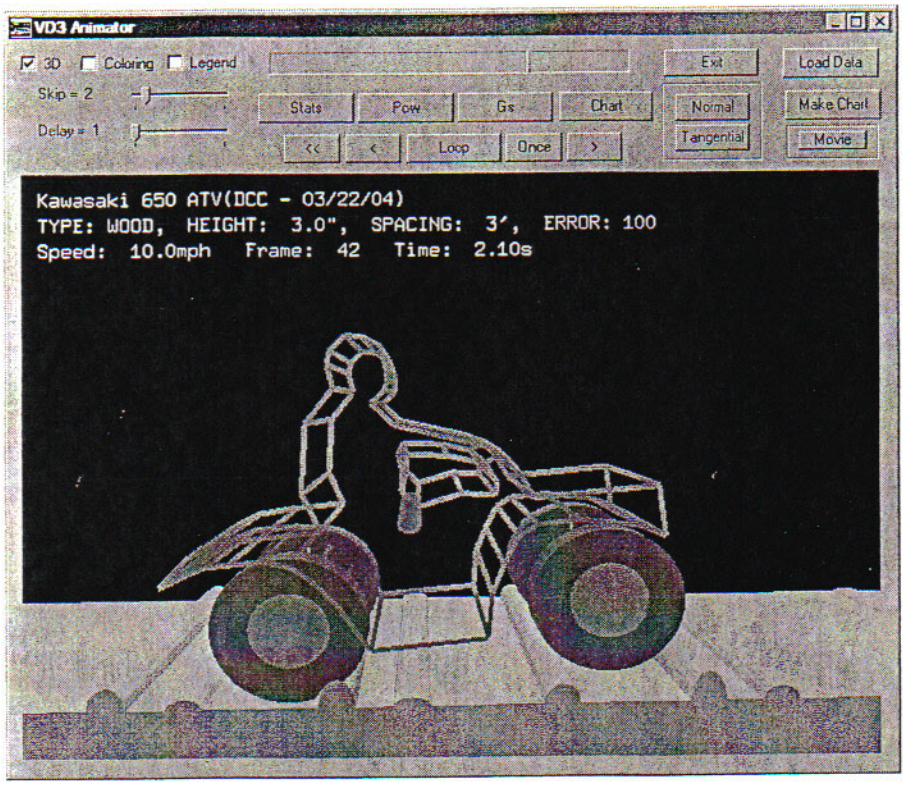

Figure 9. VEHDYN Animation of a Kawasaki 650 ATV.

Figures 10, 11 and 12,13 below shows the results of conducting simulation runs with the Vehdyn program using the same vehicle but running it over two different urban test courses with the same RMS[1] but different obstacle spacing. You can see that the results can be quite different.

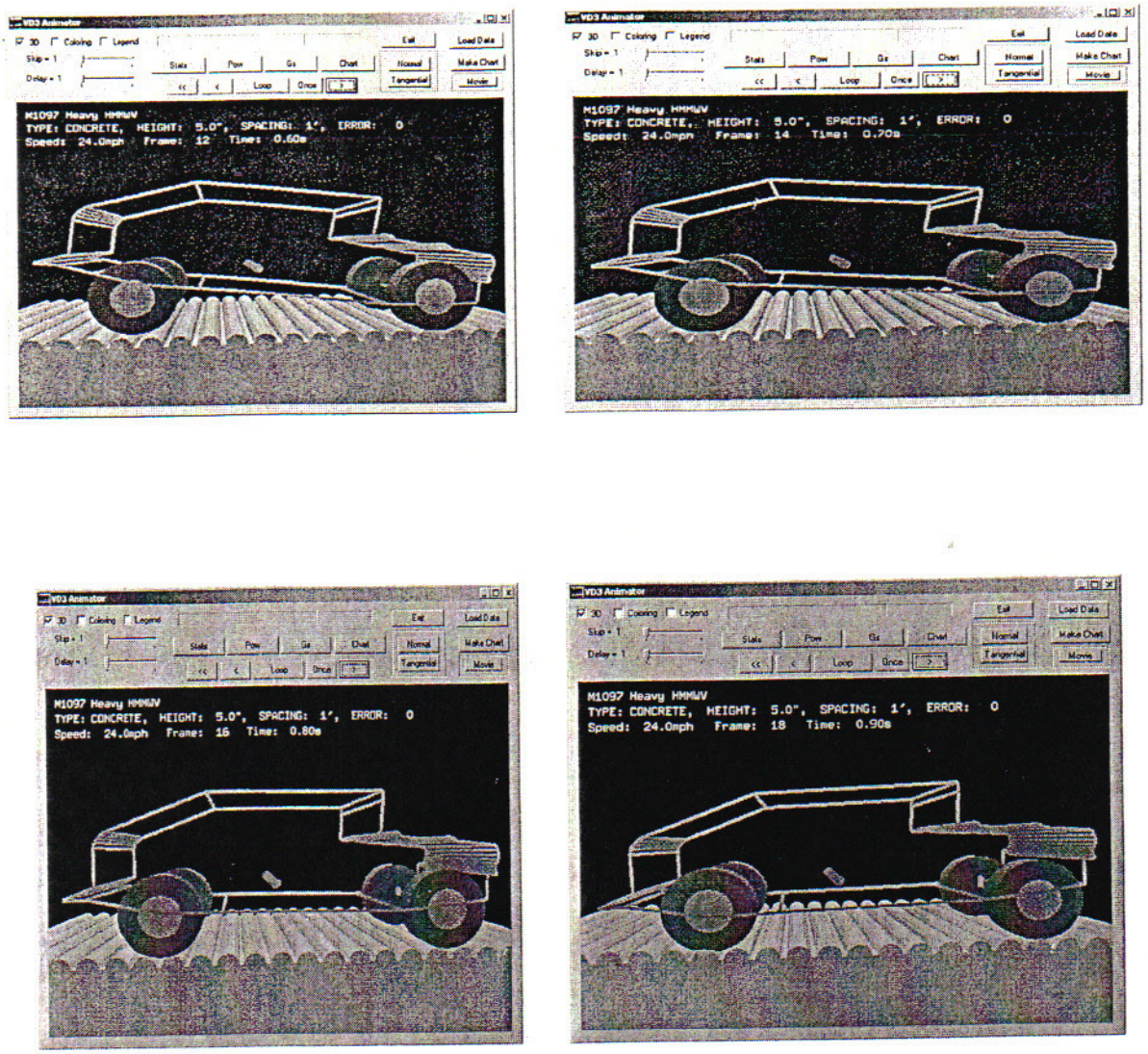

Figure 10 Time Sequenced Graphical Display of the Results of Vehdyn Simulations of the HMMV Over an Artificially Generated Urban Test Course.

[1] RMS is an acronym used in the characterization of the surface roughness of terrain, meaning root mean squared. It is determined by first detrending the surface elevation measurements taken at one foot intervals in a terrain profile and then computing the ordinary square root of the variances of the measurements from the detrended value.

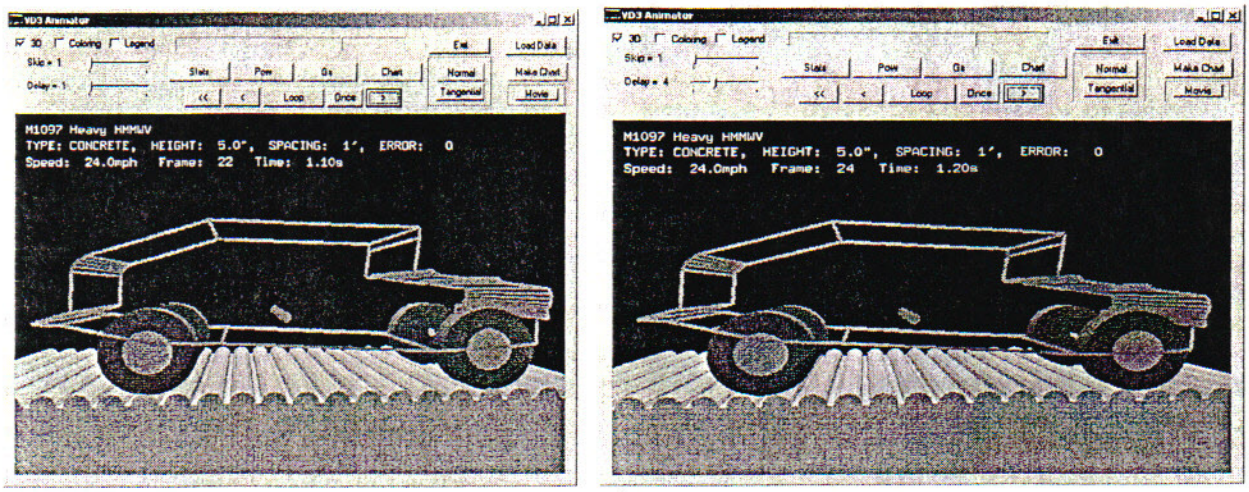

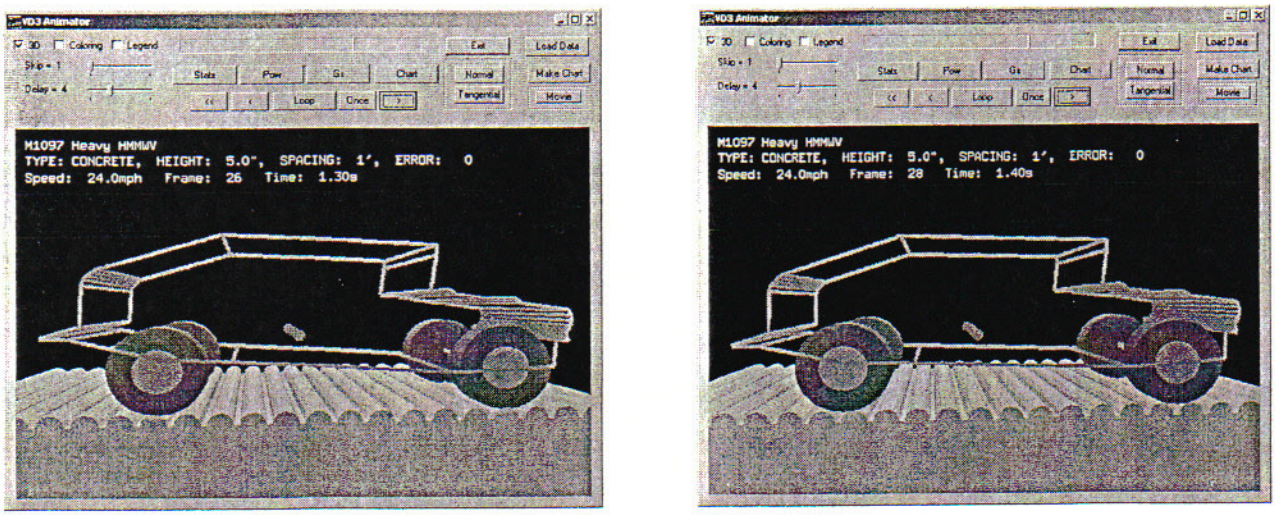

Figure 11 Continuation of the Time Sequenced Graphical Display of the Results of Vehdyn Simulations of the HMMV Over an Artificially Generated Urban Test Course.

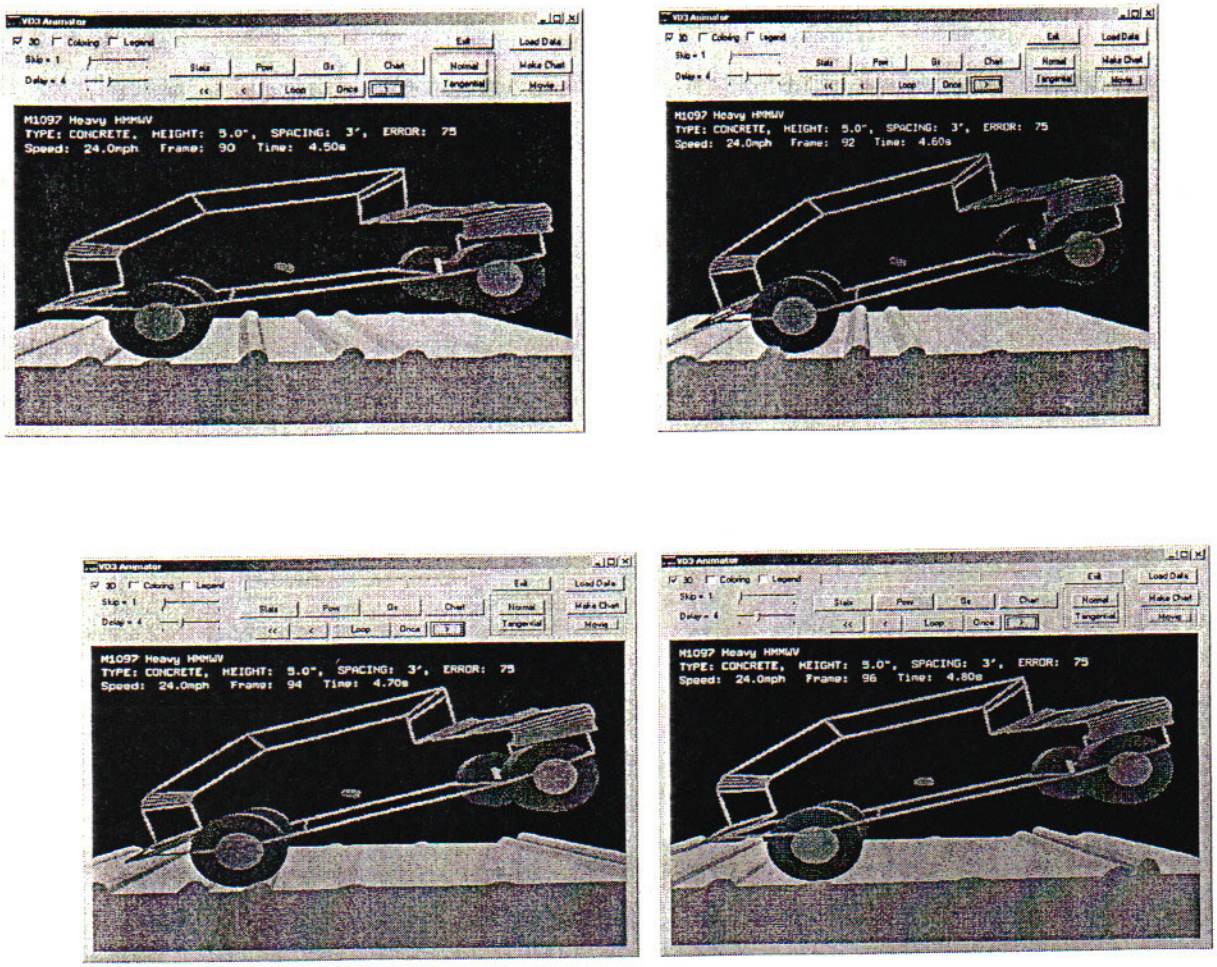

Figure 12 Time Sequenced Graphical Display of the Results of Vehdyn Simulations of the HMMV Over an Artificially Generated Urban Test Course (obstacles with different spacings).

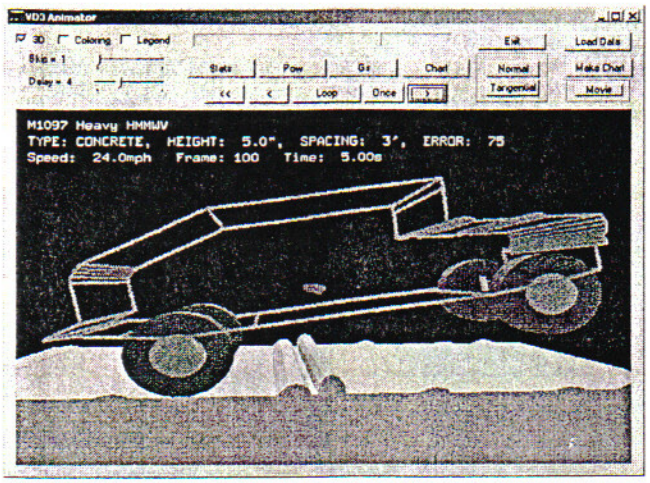

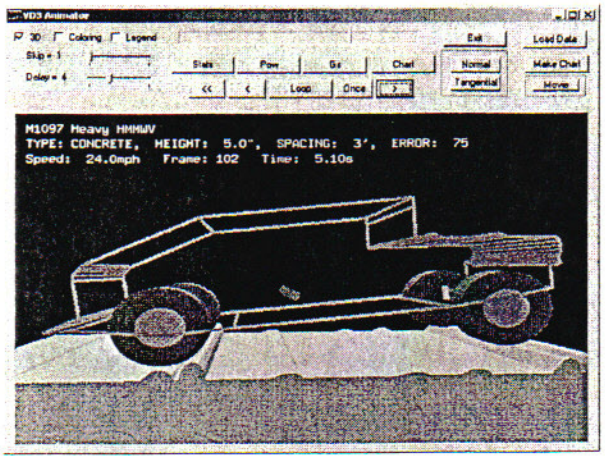

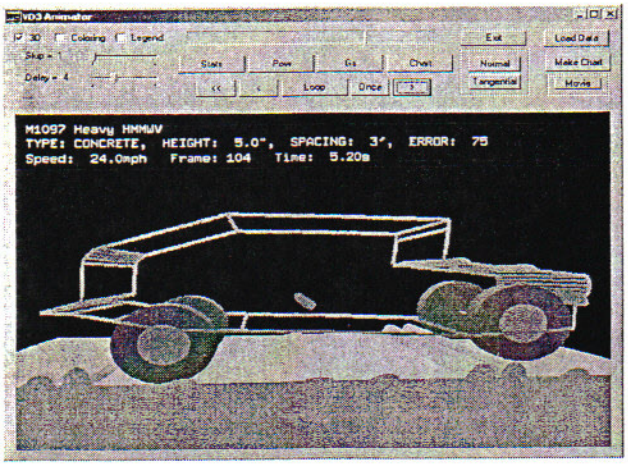

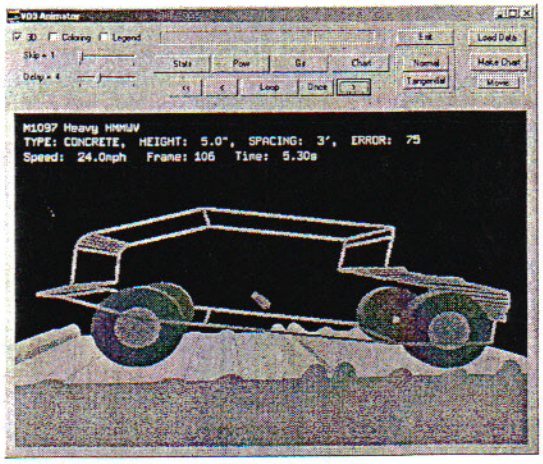

Figure 13 Continuation of a Time Sequenced Graphical Display of the Results of Vehdyn Simulations of the HMMV Over an Artificially Generated Urban Test Course (obstacles with different spacings).

METHODS

CHARACTERIZING THE TEST COURSE PROFILE SPECTRUMS USING TRANSFORMS

Transforms are the result of transforming a function of one independent variable to that of another. A common example of a transform of $f(t)$ is the cosine transform

$$f(t) = \sum_{k=0}^{\infty} A_k \cos(2\pi \frac{kt}{T}),$$

or

$$f(t) = \sum_{k=0}^{\infty} A_k \cos(2\pi\omega_k t),$$

where $\omega_k = k/T$ is the frequency. The cosine transform of $f(t)$ is literally the coefficients in the series $A_k = A(\omega_k)$ which are given by

$$A_k = \frac{2}{T}\int_0^T f(t)\cos(2\pi\omega_k t)dt .$$

Thus the function in the *time domain* is transformed to a function in *frequency domain*. The cosine transform is an example of a more general class of *linear* transforms referred to as *Fourier* transforms. Note that the transform is a *linear* combination of the sequence of cosine functions, a property of the transform, and the constant A_k a property of the data. The cosine functions are referred to as the *basis* functions or *kernel* of the transform. Other choices of basis functions give different transforms having different properties.

Consider a function as a list, or time record, of $N+1$ numbers that is a discrete sampling of a continuous function in time, $f(t)$. The readings are equally-spaced over a total time of $T=(N+1)\,\Delta t$ such that the position, k, in the list corresponds to a time equal to $k\,\Delta t$. In the discrete transform, the list of $N+1$ samples in time is transformed to a list of $N+1$ numbers, each corresponding to a discrete frequency. Each record can be computed from the summation

$$f_N = \sum_{k=0}^{N} A_k \cos(2\pi\omega_k N\Delta t) .$$

For the general discrete Fourier transforms the basis functions consist of both sines and cosines,

$$f_N = \sum_{k=0}^{N}[A_k \cos(2\pi\omega_k N\Delta t) + B_k \sin(2\pi\omega_k N\Delta t)],$$

which is generally written in *complex form* as

$$f_N = \sum_{k=-N/2}^{k=N/2} F_k \exp(i\pi\omega_k N\Delta t) .$$

The algorithm for computing this transform efficiently is referred to as the *Fast Fourier Transform.*

Estimation of the Power Spectral Density

If the profile height Y_1 is measured at equal increments Δx over a finite course length, the autocovariance function can then be computed by the formula:

$\phi_\lambda = 1/n - \lambda \sum_{i=1}^{n-\lambda} Y_i * Y_{i+\lambda}$. The corresponding estimate of the PSD is

$$P(n) = 2\Delta x(\phi_0 + 2\sum_{i=1}^{m-1} \phi_i \cos(i\lambda\pi / m) + \phi_m \cos(i\pi)\,.$$

Due to the inability to precisely resolve any frequency in a finite sample, it is necessary to smooth the spectral estimate from equation A2) over neighboring frequencies.

$\overline{P(n)} = \sum_{k=-\infty}^{\infty} A_k(\lambda) P(n-k)$ where λ is the detrending length.

The question then arises how does varying the detrending length affect the accuracy of the PSD estimation?

Table 1. Coefficients of Spectral Windows.

(Values measured as the smoothing operator moves aways from the center point-- computed in units of the detrending length)

Coefficient	Hann Values	Bartlett Values	Welch Values	Exponential Values
A_0	1	1	1	1
$A_1=A_{-1}$	.97553	.9	.99	.36788
$A_2=A_{-2}$	.90451	.8	.96	.13534
$A_3=A_{-3}$	.77389	.7	.91	.04978
$A_4=A_{-4}$	.65451	.6	.84	.01832
$A_5=A_{-5}$	.5	.5	.75	.00673
$A_6=A_{-6}$	.34549	.4	.64	.00247
$A_7=A_{-7}$	.20611	.3	.51	.00091
$A_8=A_{-8}$	.09549	.2	.36	.00033
$A_9=A_{-9}$	.024471	.1	.19	.0001
All others	<.02	0	< .15	<.0001

Why Use Transforms?

The transformed data carry the same information as the original record, whereby given the transform the original data can be retrieved. However, the transformed data are sometimes a more useful *representation*. For example, the resonant frequency of the vehicle and the roughness of the road might dominate the record of a road test. The time-domain record might not show the superposed effects whereas the two effects would be obvious in the frequency domain. *Filtering* the effect of roughness from the record amounts to removing those data from the frequency domain and transforming the result back to the time domain. *Data compression* techniques make use of the dominance of particular frequencies in a record. Compression is achieved by storing or transmitting only the F_k that are significant; decompression then is the transforming back to the time domain to obtain an approximate record that is now missing the (presumably) irrelevant data. Unfortunately, not all transforms are equally efficient. For example, a record that contains only one non-zero value (a spike) is most efficiently represented in the original time domain. In the frequency domain representation of a spike each element of the Fourier transform has the same value!

What are Wavelets

Wavelets are mathematical families of functional atoms or functional components. They can be generated from a single function ψ by dilations and translations in the form:

$\psi_{a,b} = |a|^{1/2}\psi((t-b)/a)$; where the parameters a and b are often restricted to a discrete set. In this form they provide a way to decompose an arbitrary function similar to the way sines and cosines are used in the mathematical theory of Fourier analysis. Wavelet Transforms are defined and used in wavelet methods to analyze signals in a way analogous to Fourier Transforms:

For a and b real numbers, a <>0 the discrete wavelet transform (DWT) is

$$(Tf)_m = \langle \psi_{m,n}, f \rangle = |a_0|^{-m/2} \int dt * \psi(a_0^{-m} t - nb_0) * f(t) \text{ where}$$

$$a = a_0^m \qquad b = nb_0 a_0^m$$

These methods provide an improved way to analyze and represent functions in the spatial form, the representations of which are changing with time. The book by Krantz 1999 gives a good overview of some of the mathematical topics in the theory of real analysis and functional analysis, which played a part in their invention and development.

The uses of wavelets are varied. Fournier (1995) contains an introduction to their use in computer graphics and image compression, and Charles Chu (1997) explains the uses of them to improve the functional representation by interpolation of spline of data for numerical partial differential equations. The papers by Newland and Butler, 1999 use wavelets for the study of centrifuge experiments related to earthquake engineering. The reference Torrence and Compo (1998) provides data on using them to prove the statistical significance of El Nino related sea surface temperatures.

And, corresponding to their different uses, there are many different type of wavelets: continuous wavelets (Meyer and Ryan 1993), discrete wavelets (Chu 1997), orthogonal wavelets, biorthogonal and compact wavelets (Daubechies 1992). The Daubechies scaling function, wavelet function and filter coefficients are shown in the figure below. The definitions of the scaling function and wavelet function are based on the mathematical algorithm used to compute

the wavelet decomposition by Chu 1997. The wavelet filter coefficients are the multipliers used in the wavelet transform to extract the high and low frequency components of the signal. Chu 1997 has a good reference to help understand how wavelet function, scaling function and filter coefficients work together to decompose, reconstruct, and approximate the signal.

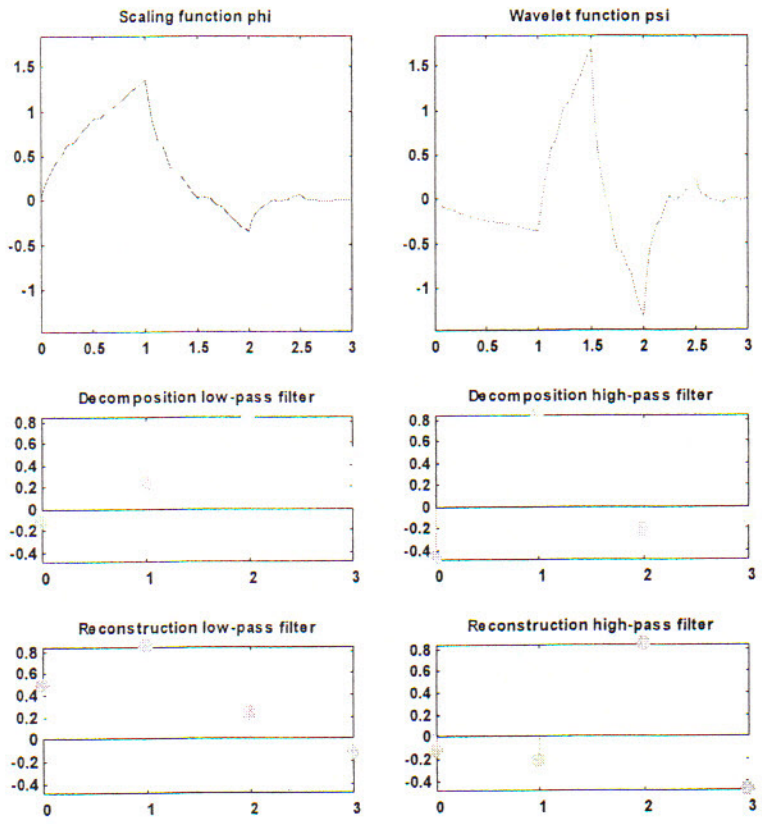

Figure 14. Example of Wavelets

The wavelet decomposition detailed process is initiated by first separating a signal s into two parts; an approximation part A1 and a detailed part D1. This is accomplished by using the coefficients of a high and low pass filter, which multiply the wavelet and scaling function. In the next level (step) the approximation A1 is itself separated into two parts A2 and D2. This process decomposition is repeated until the final level of wavelet approximation is reached.

Primarily this report we will consider Daubechies wavelets and Meyer wavelets as defined in the MATLAB wavelet toolbox (Misiti 1996), and harmonic wavelets as defined by Newland 1993. The harmonic wavelets were picked for their usefulness in analyzing time series data from vibrational studies such as those reported herein "For the purposes of signal analysis, a wavelet is considered to be a bandpass window function that stops at least the zero frequency." (Chu 1997)

Wavelet packets are a generalization of wavelets, which use two high and two low bandpass filters instead of one each (Misiti et al, 1996, Mallat 1998, Meyer and Ryan 1993,Chu 1997). Wavelet packets are more often used for one-dimensional signal analysis (as opposed to two-dimensional image compression) because they do a better job of representing the time-

dependence of the signal. They use a family of two sets of orthogonal bases to decompose the signal, instead of one. An optimal base inside of the family can be chosen that minimizes the sum of squares of residuals of the signal values and the wavelet approximation. This optimal wavelet base is often represented in terms of a particular wavelet decomposition tree. The wavelet packet decomposition process starts similarly to the wavelet decomposition process. First the s signal is separated into two parts, an approximation part A1 and a detailed part D1. This is accomplished by the coefficients of a high and low pass filter, which multiply the wavelet and scaling function. Now, in contrast to the wavelet decomposition process, in the next level (step) of the packet decomposition both the approximation A1 is separated into two parts A21 and A22 and the detailed into two parts D21 and D22. This is a composition, as mentioned above, by using two orthogonal bases for the decomposition. One base corresponds to the scaled and translated time/frequency atomic terms generated by the "mother" wavelet function. The other base corresponds to the scaled and translated time frequency atomic terms of a dual "father" wavelet function. The process is repeated until the final level of wavelet approximation is reached.

The two-dimensional plot of the square of the signal approximation in space and in time is called a Heisenberg box (Mallat 1998). These plots can be examined in order to determine the best way to subdivide the spatial and temporal axis in order to compute the wavelet bases.

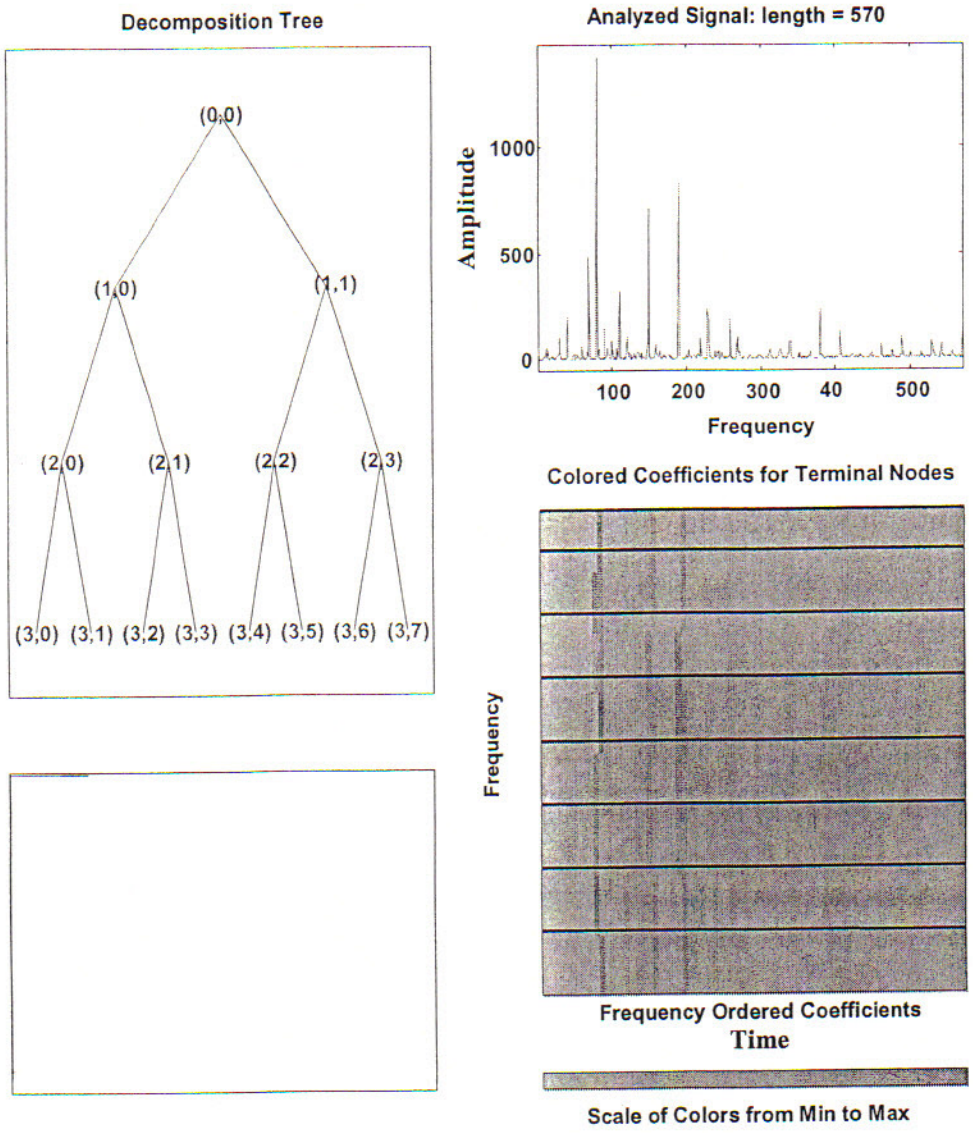

Figure 15. Example of Wavelet Decomposition

The figure above show a wavelet decomposition tree and the Heisenberg box for the decomposition of a power spectral density function. The x-axis of the signal (figure in the upper right box) is frequency and the y-axis is the square of the amplitude of the Fourier transform of the starting signal. The x-axis of the box (figure in box at lower right) is time and the y-axis is frequency. The number of boxes on the vertical y-axis corresponds to the number of frequency decomposition nodes on the lowest level in the wavelet decomposition tree.

Results

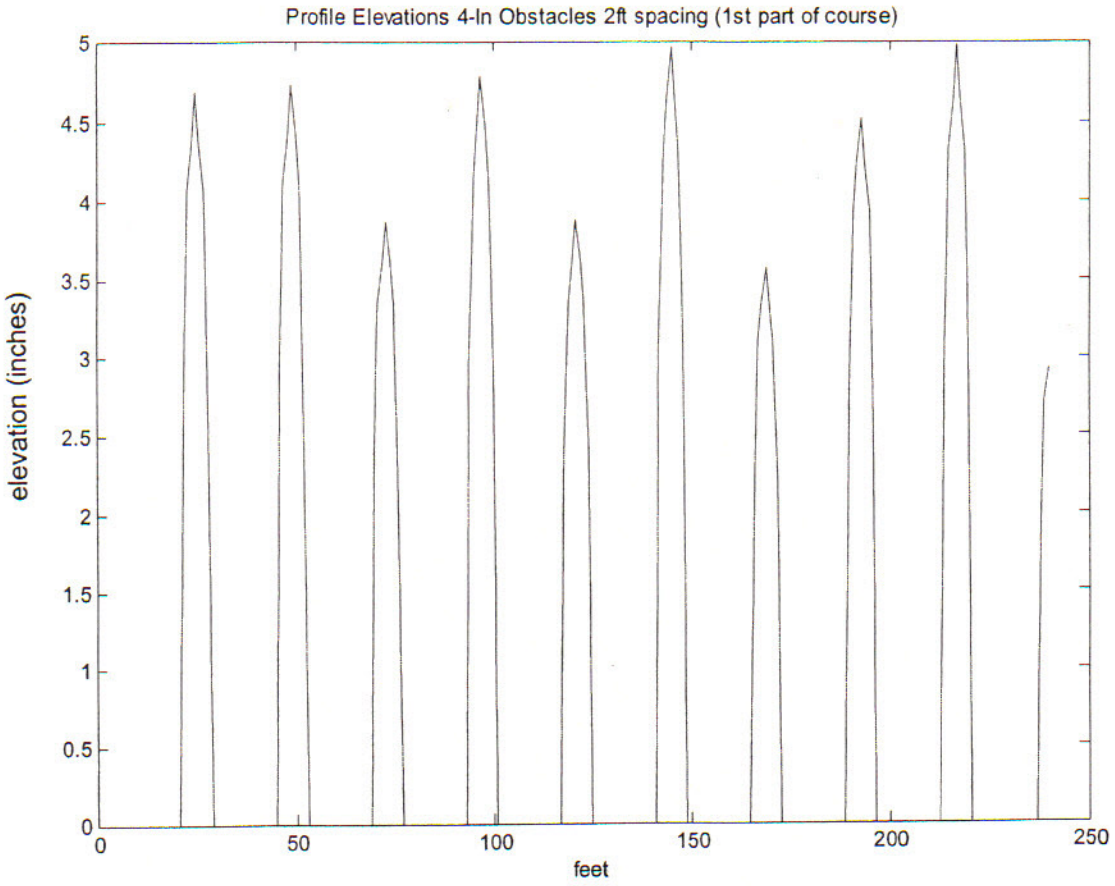

Figure 16

In appendix B there is the code for several MATLAB programs which can be used to fourier analyze the test courses. Program 1 computes the square of the fourier transform and plots a graph displaying the results. Program 2 computes a series of 10 scaled plots that display the squared fourier transform over a series of progressively larger segments of the the frequency domain. It gives an idea of how much the detail in the transform depends on the scale over which you graph the results. This is important in deciding how to differentiate and characterize the test courses. Program 3 averages the transforms using three different averaging windows or kernel transforms, the Bartlett, the Welch, and a simple unit averaging kernel. Finally, MATLAB Program 4 in Appendix B uses wavelet functions to compute various frequency transforms in order to investigate how good a job they do in characterizing the test courses.

Thus, in the figures below, which correspond to the profile in figure 16 above containing 4in obstacles at 2 ft spacing, 4 graphs are shown in order to analyze the test course. Figure 17 shows the plots made by program 1 of the scaled fourier transforms. Figure 18 shows the various, (Welch, Bartlett, square) windowed average transforms. And, Figures 19 and 20 show the wavelet analysis of the test course using Daubechie 5 and 10 discrete wavelet transforms. Each test course listed in Appendix A was analysed using this procedure and out of all the graphs computed five test courses, 1) 4' wood at 2' spacing (figures 17 and 20), 2) 1" glass at 5' spacing(figures 28,29, and 30), 3) 8" steel at 4' spacing (figures 32 and 42), and 4) 3" wood at 2' spacing (figures 38 and 20) 5) 5" concrete at 1' spacing (figures 22 and 26) were chosen to consider in this report. All the information in these analyses are shown in Figures 17 through 40 below and the results summarized in a table at the end of the paper.

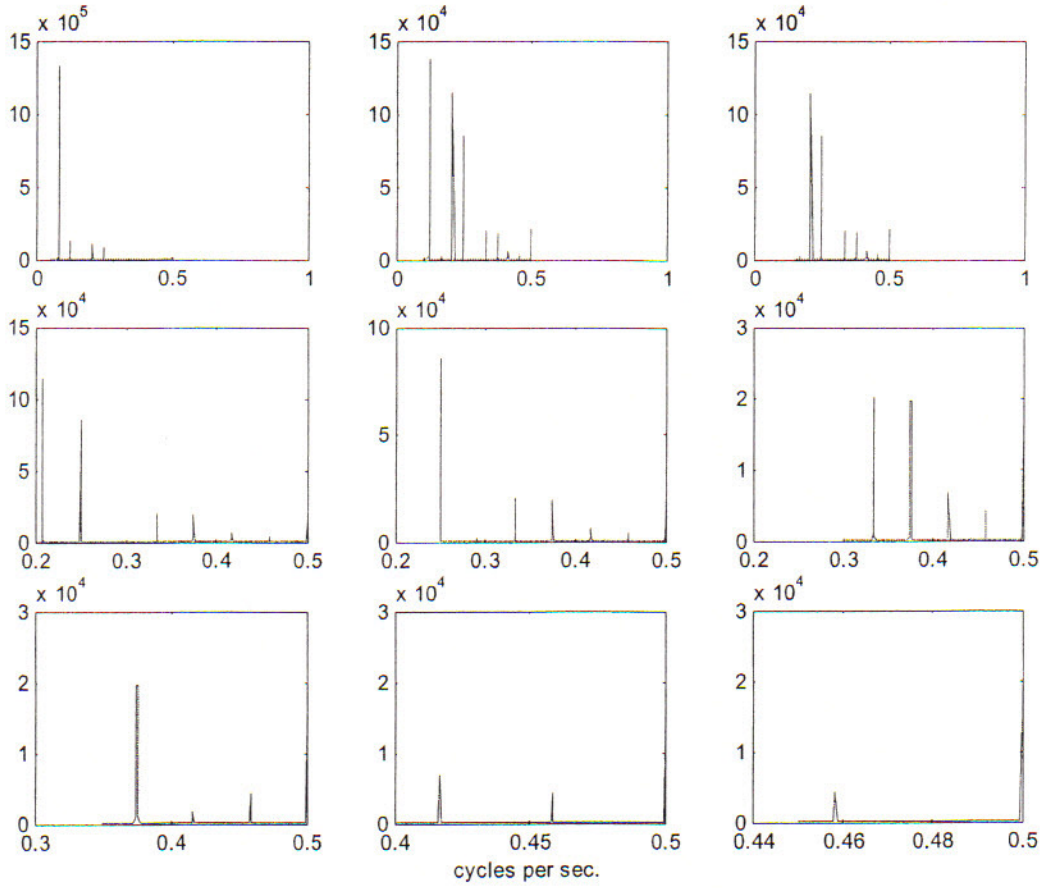

Figure 17 Scaled Power Spectrums of 4-inch Obstacles, 2' spacing

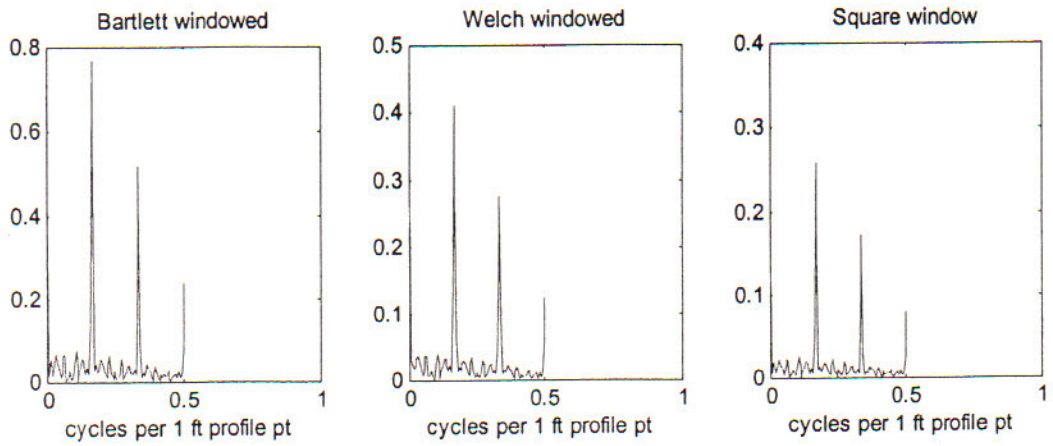

Figure 18 Windowed Power Spectrum of 4' wood debris field at 2 ft spacings